TECHNICAL REPORT
NATICK/TR-96/004

AD_____

EXPERIMENTAL UNCERTAINTY IN THIRD-ORDER SUSCEPTIBILITY AND MOLECULAR SECOND HYPERPOLARIZABILITY MEASUREMENTS OBTAINED WITH DEGENERATE FOUR-WAVE MIXING

By

Brian R. Kimball
and
Joseph F. Roach

December 1995

Final Report

March 1994 - November 1994

Approved for public release, distribution unlimited

UNITED STATES ARMY SOLDIER SYSTEMS COMMAND
NATICK RESEARCH, DEVELOPMENT AND ENGINEERING CENTER
NATICK, MASSACHUSETTS 01760-5020

DISCLAIMERS

The findings contained in this report are not to be construed as an official Department of the Army position unless so designated by other authorized documents.

Citation of trade names in this report does not constitute an official endorsement or approval of the use of such items.

DESTRUCTION NOTICE

For Classified Documents:

Follow the procedures in DoD 5200.22-M, Industrial Security Manual, Section II-19 or DoD 5200.1-R, Information Security Program Regulation, Chapter IX.

For Unclassified/Limited Distribution Documents:

Destroy by any method that prevents disclosure of contents or reconstruction of the document.

REPORT DOCUMENTATION PAGE

Form Approved
OMB No. 0704-0188

1. AGENCY USE ONLY (Leave blank)	2. REPORT DATE	3. REPORT TYPE AND DATES COVERED
	December 1995	FINAL - March 1994 - November 1994

4. TITLE AND SUBTITLE
Experimental Uncertainty in Third-Order Susceptibility and Molecular Second Hyperpolarizability Measurements Obtained with Degenerate Four-Wave Mixing

5. FUNDING NUMBERS
AgC: TB1089PE
PR: 1L1AH980
TA: CAOAOO

6. AUTHOR(S)
Brian R. Kimball and Joseph F. Roach

7. PERFORMING ORGANIZATION NAME(S) AND ADDRESS(ES)
U.S. Army Soldier Systems Command
Natick RD&E Center
Kansas St. ATTN: AMSSC-YSD
Natick, MA 01760-5020

8. PERFORMING ORGANIZATION REPORT NUMBER
NATICK/TR-96/004

9. SPONSORING / MONITORING AGENCY NAME(S) AND ADDRESS(ES)

10. SPONSORING / MONITORING AGENCY REPORT NUMBER

11. SUPPLEMENTARY NOTES

12a. DISTRIBUTION / AVAILABILITY STATEMENT
Approved for public release, distribution unlimited

12b. DISTRIBUTION CODE

13. ABSTRACT *(Maximum 200 words)*

An uncertainty analysis is performed on a degenerate four-wave mixing scheme used in the determination of the third-order susceptibility and molecular second hyperpolarizability of nonlinear optical materials. Equations are derived based on the root-sum-squares method, which accounts for uncertainty in all applicable experimental parameters. These expressions are incorporated into a computer program, which is used to investigate absolute and relative uncertainties as well as the sensitivity of overall system accuracy to individual parameters. Conclusions are drawn based on the results of the analysis.

14. SUBJECT TERMS			15. NUMBER OF PAGES
THIRD -ORDER SUSCEPTIBILITY	THIRD-ORDER NONLINEARITIES	OPTICAL NONLINEARITY	45
NONLINEAR OPTICAL MATERIALS	FOUR-WAVE MIXING	LASER EYE PROTECTION	16. PRICE CODE
DEGENERATE FOUR-WAVE MIXING	STATISTICAL ANALYSIS	UNCERTAINTY ANALYSIS	

17. SECURITY CLASSIFICATION OF REPORT	18. SECURITY CLASSIFICATION OF THIS PAGE	19. SECURITY CLASSIFICATION OF ABSTRACT	20. LIMITATION OF ABSTRACT
Unclassified	Unclassified	Unclassified	

TABLE OF CONTENTS

LIST OF FIGURES

LIST OF TABLES

PREFACE

This report summarizes the development and application of an analysis of the uncertainty in third-order susceptibility and second hyperpolarizability measurements obtained experimentally with degenerate four-wave mixing. This work is being done under the project Laser Eye Protection, 5325006CA0A00, administered by the Technology Application Branch, Fiber and Polymer Science Division, Science and Technology Directorate, U.S. Army Soldier Systems Command, Natick Research, Development, and Engineering Center.

All experiments were performed at the Technology Application Branch, at the Natick Research, Development, and Engineering Center (Natick). The citation of trade names in this report does not constitute official endorsement or approval of use of an item.

EXPERIMENTAL UNCERTAINTY IN THIRD-ORDER SUSCEPTIBILITY AND MOLECULAR SECOND HYPERPOLARIZABILITY MEASUREMENTS OBTAINED WITH DEGENERATE FOUR WAVE MIXING

INTRODUCTION

Third-order susceptibility and molecular second hyperpolarizability measurements are currently performed with degenerate four-wave mixing (DFWM). Experimental values obtained by this technique have been reported with estimated confidence intervals. This report describes an uncertainty analysis that can be used to 1) better define experimental uncertainties, 2) add some insight into the degree to which individual experimental parameters affect overall system accuracy, and 3) validate comparisons of experimental $\chi^{(3)}$ and $\langle\gamma\rangle$ values for various compounds to confirm the significance of any observed variations in nonlinear response, as in the study of trends.

The DFWM system described here utilizes a backward-beam geometry where two strong collinear pump beams, propagating in opposite directions, interact at the sample with a third less-intense probe beam to create a fourth nonlinear optical phase conjugate beam. The intensity of the conjugate signal is proportional to the square of the $\chi^{(3)}$ of the sample under study. The signal is measured with a silicon photodiode and oscilloscope. It is then compared to a similar signal obtained from a carbon disulfide standard under identical conditions using the expression

$$\frac{\chi^{(3)}_{sample}}{\chi^{(3)}_{CS_2}} = \left(\frac{n_{sample}}{n_{CS_2}}\right)^2 \frac{d\alpha}{1-e^{-\alpha d}} e^{\alpha d/2} \left(\frac{I_{sample}}{I_{CS_2}}\right)^{1/2} \frac{d_{CS_2}}{d_{sample}} \cdots \qquad (1)$$

where n is the index of refraction, α is the linear absorption coefficient, d is the length of the sample and I is the measured signal of the phase conjugate beam. This approach eliminates the need of obtaining absolute irradiance measurements for each of the additional three beams used in the DFWM setup.[1]

The relationship between the molecular second hyperpolarizability $\langle\gamma\rangle$ and the third-order macroscopic susceptibility of the solute is given by the expression

$$\langle\gamma\rangle = \frac{\chi^{(3)}}{L^4 N} \qquad (2)$$

where N is the number density of molecules per mL and

$$L = \frac{n^2+2}{3}. \tag{3}$$

It is generally assumed that the conjugate signal is due to a combination of third-order nonlinearities in both the solvent and solute and that for a solution of noninteracting particles the relationship is additive:[1]

$$\chi^3_{solution} = L^4[N_{solvent}\gamma_{solvent} + N_{solute}\gamma_{solute}]\cdots \tag{4}$$

The $\chi^{(3)}_{solution}$ is obtained experimentally with Eq. 1. For nonsaturated solutions

$$N_{solute} = \frac{AC}{M} \tag{5}$$

where A is Avogadro's number, M is the molecular weight of the solute, and C is the concentration. Making appropriate substitutions of Eqs. 2 and 5 into Eq. 4, the following expression is obtained:

$$\chi^3_{solution} = \chi^3_{solvent} + (L^4 \gamma_{solute} A/M)\, C. \tag{6}$$

By evaluating Eq. 1 for a series of dilute solutions and plotting the results versus respective concentration, a straight line is obtained. A least-squares approximation is then applied to the data from which one obtains $\chi^{(3)}_{solvent}$ from the y-intercept and γ_{solute} from the slope. The $\chi^{(3)}_{solute}$ is then obtained from Eq. 2.

DERIVATION OF UNCERTAINTY EQUATIONS

If it is assumed that the uncertainties (W_1, W_2,...,W_n) in the independent variables (X_1, X_2,...,X_n) are all given with the same probability, then the uncertainty (W_R) in the dependent variable (R) is given by the expression

$$W_R = \left[\left(\frac{(\partial R)}{\partial X_1} W_1\right)^2 + \left(\frac{(\partial R)}{\partial X_2} W_2\right)^2 + \ldots + \left(\frac{(\partial R)}{\partial X_N} W_N\right)^2\right]^{1/2}. \tag{7}$$

By inserting Eq. 1 into Eq. 7 a probable estimate of the uncertainty in experimentally determined $\chi^{(3)}_{sample}$ is obtained:

$$W_{\chi^{(3)}_s} = \left[\left(\frac{\partial \chi^{(3)}_s}{\partial \chi^{(3)}_R} W_{\chi^3}\right)^2 + \left(\frac{\partial \chi^{(3)}_s}{\partial I_s} W_{I_s}\right)^2 + \left(\frac{\partial \chi^{(3)}_s}{\partial I_R} W_{I_R}\right)^2 + \left(\frac{\partial \chi^{(3)}_s}{\partial n_s} W_{n_s}\right)^2 + \left(\frac{\partial \chi^{(3)}_s}{\partial n_R} W_{n_R}\right)^2 + \left(\frac{\partial \chi^{(3)}_s}{\partial d_R} W_{d_R}\right)^2 + \left(\frac{\partial \chi^{(3)}_s}{\partial d_s} W_{d_s}\right)^2 + \left(\frac{\partial \chi^3(3)_s}{\partial \alpha} W_\alpha\right)^2\right]^{1/2}, \tag{8}$$

where

$$\frac{\partial \chi^{(3)}_s}{\partial \chi^{(3)}_R} = \left(\frac{I_s}{I_R}\right)^{1/2}\left(\frac{n_s}{n_R}\right)^2\left(\frac{d_R}{d_s}\right)\frac{\alpha L}{(1-e^{-\alpha L})} e^{\alpha L/2}, \tag{9}$$

$$\frac{\partial \chi^{(3)}_s}{\partial I_s} = \frac{\chi^{(3)}_R}{2\sqrt{I_s I_R}}\left(\frac{n_s}{n_R}\right)^2\left(\frac{d_R}{d_s}\right)\frac{\alpha L}{(1-e^{-\alpha L})} e^{\alpha L/2}, \tag{10}$$

$$\frac{\partial \chi^{(3)}_s}{\partial I_R} = \frac{-\chi^{(3)}_R}{2}\frac{(I_s)^{1/2}}{(I_R)^{3/2}}\left(\frac{n_s}{n_R}\right)^2\left(\frac{d_R}{d_s}\right)\frac{\alpha L}{(1-e^{-\alpha L})} e^{\alpha L/2}, \tag{11}$$

$$\frac{\partial \chi^{(3)}_s}{\partial n_s} = \chi^{(3)}_R\left(\frac{I_s}{I_R}\right)^{1/2}\left(\frac{2n_s}{n_R^2}\right)\left(\frac{d_R}{d_s}\right)\frac{\alpha L}{(1-e^{-\alpha L})} e^{\alpha L/2}, \tag{12}$$

$$\frac{\partial \chi^{(3)}_s}{\partial n_R} = \chi^{(3)}_R\left(\frac{I_s}{I_R}\right)^{1/2}\left(\frac{-2n_s^2}{n_R^3}\right)\left(\frac{d_R}{d_s}\right)\frac{\alpha L}{(1-e^{-\alpha L})} e^{\alpha L/2}, \tag{13}$$

$$\frac{\partial \chi^{(3)}{}_S}{\partial d_R} = \chi^{3)}{}_R \left(\frac{I_s}{I_R}\right)^{1/2} \left(\frac{n_s}{n_R}\right)^2 \left(\frac{1}{d_s}\right) \frac{\alpha L}{(1-e^{-\alpha L})} e^{\alpha L/2}, \tag{14}$$

$$\frac{\partial \chi^{(3)}{}_S}{\partial d_s} = \chi^{(3)}{}_R \left(\frac{I_s}{I_R}\right) \left(\frac{n_s}{n_R}\right)^2 \left(\frac{-d_R}{d_s^2}\right) \frac{\alpha L}{(1-e^{-\alpha L})} e^{\alpha L/2}, \tag{15}$$

and

$$\frac{\partial \chi^{(3)}{}_S}{\partial \alpha} = \chi^{(3)}{}_R \left(\frac{I_s}{I_R}\right)^{1/2} \left(\frac{n_s}{n_R}\right)^2 \left(\frac{d_R}{d_s}\right) \frac{(1-e^{-\alpha L})\left[L\left(\frac{\alpha L}{2}+e^{\alpha L/2}\right)\right]-\alpha L^2 e^{-\alpha L/2}}{(1-e^{-\alpha L})^2}. \tag{16}$$

Similarly, for the uncertainty in $\langle \gamma \rangle$, Eq. 2 is applied to Eq. 7 to obtain:

$$W_\gamma = \left[\left(\frac{\partial \gamma}{\partial \chi^{(3)}} W_{\chi^{(3)}}\right)^2 + \left(\frac{\partial \gamma}{\partial M} W_M\right)^2 + \left(\frac{\partial \gamma}{\partial L} W_L\right)^2 + \left(\frac{\partial \gamma}{\partial A} W_A\right)^2\right]^{1/2}, \tag{17}$$

where

$$\frac{\partial \gamma}{\partial \chi^{(3)}} = \frac{M}{L^4 A}, \tag{18}$$

$$\frac{\partial \gamma}{\partial M} = \frac{\chi^{(3)}}{L^4 A}, \tag{19}$$

$$\frac{\partial \gamma}{\partial L} = \frac{-4\chi^{(3)} M}{L^5 A}, \tag{20}$$

and

$$\frac{\partial \gamma}{\partial A} = 0 \quad (\textit{assumed}). \tag{21}$$

In order to evaluate Eq. 8, absolute error values are required for $\chi^{(3)}{}_R$, I_S, I_R, n_S, n_R, d_R, d_S, and α. These can all be determined directly through

experimental considerations or can be given assumed values. For Eq. 17 error values for M, $\chi^{(3)}$ (solute), and L must be obtained. Additional calculations must be performed to obtain estimates for the uncertainty in $\chi^{(3)}$ (solute), and L. For W_L, Eqs 3 and 7 are combined:

$$W_L = \left[\left(\frac{\partial L}{\partial n_s} W_{n_s}\right)^2\right]^{1/2}, \tag{22}$$

where

$$\frac{\partial L}{\partial n_s} = \frac{2n_s}{3}. \tag{23}$$

For the uncertainty in $\chi^{(3)}$, Eq. 6 is first written in the form:

$$\chi^{(3)}{}_{slt} = \frac{(\chi^{(3)}{}_s - \chi^{(3)}{}_{slv})\ (1000)}{C}. \tag{24}$$

The factor of 1000 is included as a dimensional constant. Applying Eq. 7:

$$W_{\chi^{(3)}{}_{slt}} = \left[\left(\frac{\partial \chi^{(3)}{}_{slt}}{\partial \chi^{(3)}{}_s} W_{\chi^{(3)}{}_s}\right)^2 + \left(\frac{\partial \chi^{(3)}{}_{slt}}{\partial \chi^{(3)}{}_{slv}} W_{\chi^{(3)}{}_{slv}}\right)^2 + \left(\frac{\partial \chi^{(3)}{}_{slt}}{\partial C} W_C\right)^2\right]^{1/2}, \tag{25}$$

where

$$\frac{\partial \chi^3{}_{slt}}{\partial \chi^3{}_s} = \frac{1000}{C}, \tag{26}$$

$$\frac{\partial \chi^3{}_{slt}}{\partial \chi^3{}_{slv}} = \frac{-1000}{C}, \tag{27}$$

and

$$\frac{\partial \chi^3{}_{slt}}{\partial \chi^3{}_{slv}} = 1000\left(\frac{\chi^{(3)}{}_s - \chi^{(3)}{}_{slv}}{C^2}\right). \tag{28}$$

The value of W_C depends upon the method with which the solutions are prepared. The technique currently being used relies on accurate weight measurements to determine the solution concentration. Briefly, an initial concentration (C_i) is prepared using a precision balance for the solute and a volumetric flask for the solvent. For each run a portion of the solution is used. After each run the mass of the remaining solution is determined (m_f). The flask is again filled and weighed to obtain the initial weight of the next run (m_n). Using the following expression the new concentration is obtained (see Appendix A for derivation):

$$C_n = C_i \frac{m_f}{m_n}. \tag{29}$$

Advantages of this technique include ease of weight measurements, a reduction in waste solvent, and high overall accuracy. To obtain W_C we evaluate the following equation:

$$W_{C_n} = \left[\left(\frac{\partial C_n}{\partial C_i} W_{C_i}\right)^2 + \left(\frac{\partial C_n}{\partial m_f} W_{m_f}\right)^2 + \left(\frac{\partial C_n}{\partial m_n} W_{m_n}\right)^2\right]^{1/2}, \tag{30}$$

where

$$\frac{\partial C_n}{\partial C_i} = \frac{m_f}{m_n}, \tag{31}$$

$$\frac{\partial C_n}{\partial m_f} = \frac{C_i}{m_n}, \tag{32}$$

and

$$\frac{\partial C_n}{\partial m_n} = \frac{-C_i m_f}{m_n^2}. \tag{33}$$

In order to evaluate Eq. 30 a value for W_{Ci} must be estimated. Beginning with the expression

$$C_i = \frac{m_i}{V_i}, \tag{34}$$

where m_i is the initial weight and V_i is the initial volume, we must evaluate the following equation:

$$W_{C_i} = \left[\left(\frac{\partial C_i}{\partial m_i} W_{m_i}\right)^2 + \left(\frac{\partial C_i}{\partial V_i} W_{V_i}\right)^2\right]^{1/2}, \tag{35}$$

where

$$\frac{\partial C_i}{\partial m_i} = \frac{1}{V_i}, \tag{36}$$

and

$$\frac{\partial C_i}{\partial V_i} = \frac{-m_i}{V_i^2}. \tag{37}$$

These expressions have been incorporated into a computer program (Appendix B) which calculates $\chi^{(3)}_{solution}$, $\chi^{(3)}_{solute}$, and $\langle\gamma\rangle_{solute}$ and the uncertainties associated with each of these values.

EXPERIMENTAL-PARAMETER SENSITIVITY

In order to evaluate the uncertainty equations that were derived in the previous section, values are assumed for the absolute errors of the independent variables. These are given as percent errors in Table 1.

Table 1. Assumed percent errors for experimental parameters

Parameter	Assumed Percent Error
$\chi^{(3)}_{CS2}$	0%
$I_{solution}$	5%
I_{CS2}	5%
$n_{solution}$	1%
n_{CS2}	0.1%
d_{sample}	0.1%
d_{CS2}	0.1%
$\alpha_{solution}$	0.08%
M_{solute}	0.1%
$mass_{solution}$	1%
$volume_{solution}$	1%

It is assumed that an exact value for $\chi^{(3)}_{CS2}$ is known. Uncertainties in intensity measurements are based on an estimate of the readability of the oscilloscope used in the evaluations. The index of refraction for CS_2 is considered more accurate than that of the sample because it is assumed that $n_{solution} = n_{solvent}$, and additional error is allowed here. Percent errors given for the cell thicknesses d_{sample} and d_{CS2} are manufacturer stated tolerances. Mass and volume tolerances are based on scale readabilities.

Absolute errors for solution concentrations are calculated using Eq. 30. These will slightly increase with each new solution that is prepared. For example, for an initial concentration of 1 mg/mL, where 0.005 g of solute is dissolved in 5 mL of solvent with tolerances of ±0.0001 g and ± 0.05 mL, respectively, Eq. 35 gives an uncertainty of 0.00002 g/mL or 2.2% for the initial concentration. This value is then used as input into Eq. 30 to obtain the uncertainty in the following, more dilute solution. Table 2 shows an example in which each consecutive concentration is half the previous concentration. New concentrations (C_n) are calculated at the end of each run using the mass measurements shown for that run and Eq. 29. Absolute uncertainties (W_{Cn}) are predicted with Eq. 30 and percent errors are also shown for each run.

Table 2. Uncertainty in concentration measurements for a standard run.

C_i (g/mL)	m_i (g)	m_f (g)	m_n (g)	C_n (g/mL)	W_{Cn} (g/mL)	% Error
1×10^{-3}	4.6	2.3	4.6	5×10^{-4}	1×10^{-5}	1%
5×10^{-4}	4.6	2.3	4.6	2.5×10^{-4}	5×10^{-6}	1%
2.5×10^{-4}	4.6	2.3	4.6	1.25×10^{-4}	4×10^{-6}	1.6%
1.25×10^{-4}	4.6	2.3	4.6	6.25×10^{-5}	2×10^{-6}	1.6%
6.25×10^{-5}	4.6	2.3	4.6	3.12×10^{-5}	1×10^{-6}	1.6%

These values are used as input to program ERRCHI-3.BAS. Table 3 gives additional input for a representative run where the $\chi^{(3)}$ of zinc tetraphenyl tetrabenzporphyrin in tetrahydrafuran was evaluated.

Table 3. ERRCHI-3.BAS input data for experimental run of zinc tetraphenyl tetrabenzporphyrin in tetrahydrafuran.

Variable	Input
$I_{solution}$	28000
I_{CS2}	150000
$\propto$	0.875
C_i	0.00076 g/mL
$\chi^{(3)}_{solvent}$	2.4×10^{-14} esu
$W_{\chi(3)solvent}$	9.7×10^{-16} esu
M	678
weight	0.0038 g
vol	5 mL

The following output was obtained for this run:

$\chi^{(3)}$ of solution = 1.45×10^{-12}
Uncertainty = 5.94×10^{-14}
Percent Error = 4%

$\chi^{(3)}$ of solute = 1.88×10^{-9}
Uncertainty = 7.85×10^{-11}
Percent Error = 4%

$\langle\gamma\rangle$ of solute = 6.3×10^{-31}
Uncertainty = 3.64×10^{-32}
Percent Error = 6%

Uncertainty in $\chi^{(3)}_{solution}$ due to:
$\chi^{(3)}_{CS2} = 0$
Voltage reading for solution = 3.6×10^{-14}
Voltage reading for CS_2 = 3.6×10^{-14}
Solution refractive index = 2.9×10^{-14}
CS_2 refractive index = 2.9×10^{-15}
Solution cell thickness = 1.5×10^{-15}
CS_2 cell thickness = 1.5×10^{-15}
Sample absorption = 5.4×10^{-16}

Uncertainty in concentration due to:
Weight = 0.0076
Volume = 0.0076

Uncertainty in $\chi^{(3)}_{solute}$ due to:
$\chi^{(3)}_{solution} = 7.8\times10^{-11}$
$\chi^{(3)}_{solvent} = 1.3\times10^{-11}$
Concentration = 2.7×10^{-11}

Uncertainty in field factor due to:
Solution refractive index = 0.014

Uncertainty in $\langle\gamma\rangle$ due to:
$\chi^{(3)}_{solute} = 2.7\times10^{-32}$
Molecular weight = 6.3×10^{-34}
Field factor (L) = 2.5×10^{-32}

The value for $\chi^{(3)}_{solvent}$ and its corresponding uncertainty was obtained by first running the program at zero concentration. Uncertainties due to individual experimental parameters shown above are obtained from the product of the parameter sensitivity and its absolute uncertainty, for instance, from Eq. 7:

$$\frac{\partial R}{\partial X_1} W_1. \qquad (38)$$

These values show the relative degree to which single variables contribute to the overall uncertainty. For example, the greatest degree of uncertainty in the experimental value for $\chi^{(3)}_{solution}$ is due to oscilloscope voltage readings.

A similar output to that shown above is obtained for each concentration evaluated in the series. Each value of $\chi^{(3)}_{solution}$, $\chi^{(3)}_{solute}$, and $\langle\gamma\rangle$ will have an associated uncertainty based on the values of the experimental parameters unique to that run. The final values reported for $\chi^{(3)}_{solution}$, $\chi^{(3)}_{solute}$, and $\langle\gamma\rangle$ are obtained via a curve fitting technique while their respective uncertainties are obtained by taking the sample standard deviation of the individual uncertainties obtained for each run.

In some instances the input uncertainties given in Table 1 may vary; for example, in a case where the sample is in the form of a thin film, the thickness of which can only be approximated. With this in mind a series of plots were generated which show the change in the uncertainty of $\chi^{(3)}_{solute}$ and $\langle\gamma\rangle$ resulting from an increase in the uncertainty of a single variable. These are shown in Appendix C, Figs. C1-C21. In each plot the uncertainty in a single independent variable has been increased from 0% to 50% error while the uncertainty in the remaining independent variables has been kept constant at the current values.

The series of sensitivity plots for both $\chi^{(3)}_{solute}$ and $\langle\gamma\rangle$ are summarized in the following bar charts where the normalized average slope of each variable is shown. The charts show the relative degree to which a given variable is sensitive to changes in percent error. For example, the uncertainty in $\chi^{(3)}_{solute}$ is most sensitive to uncertainty in the refractive indices of both CS_2 and the solution while accuracy in determining the linear absorption of the sample has a minimal effect.

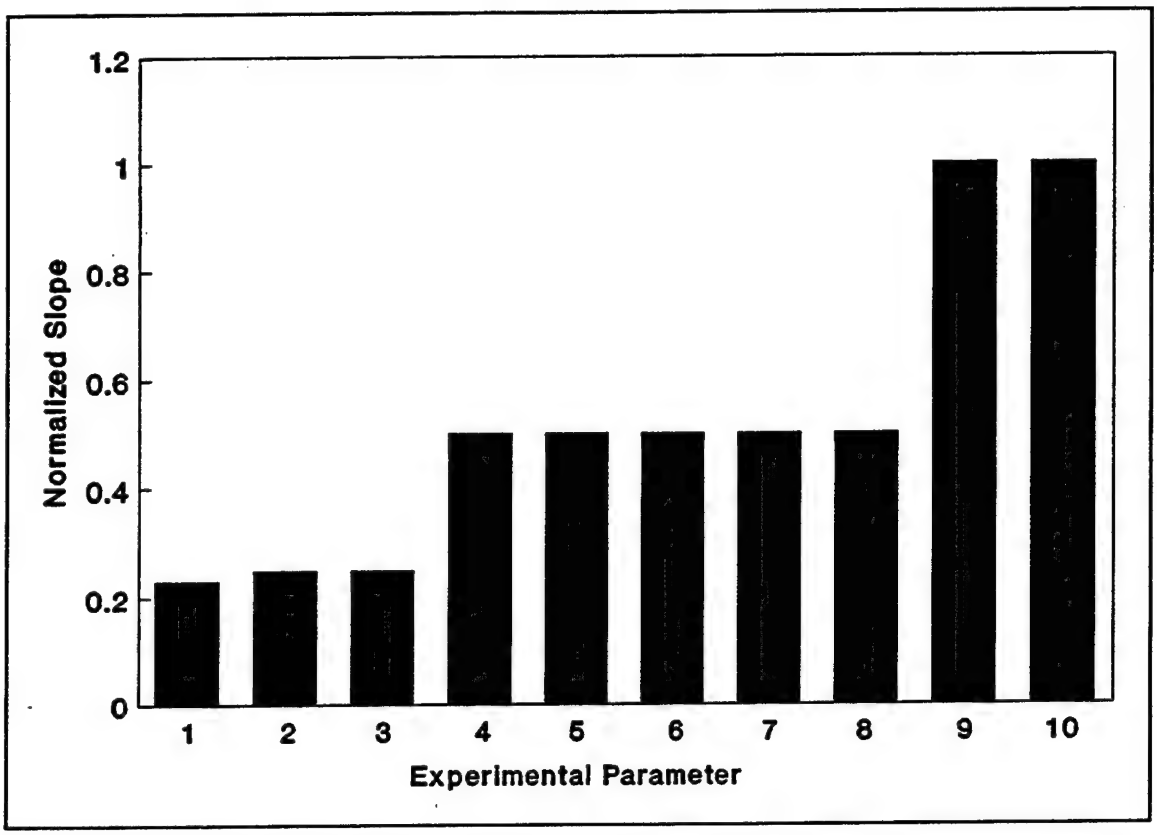

Fig. 1. Normalized average slopes of parameter sensitivity curves for $\chi^{(3)}_{solute}$.

Parameters shown in Fig. 1:

1 -- Sample absorption
2 -- $I_{solution}$
3 -- I_{CS2}
4 -- $\chi^{(3)}_{CS2}$
5 -- Sample thickness
6 -- CS_2 thickness
7 -- Sample mass
8 -- Sample volume
9 -- n_{CS2}
10-- $n_{solution}$

Figure 2 shows that $\langle\gamma\rangle$ is also most sensitive to uncertainty in the refractive indices of CS_2 and sample solution. The increased dependence on $n_{solution}$ is due to its presence in the local field factor (Equation 3).

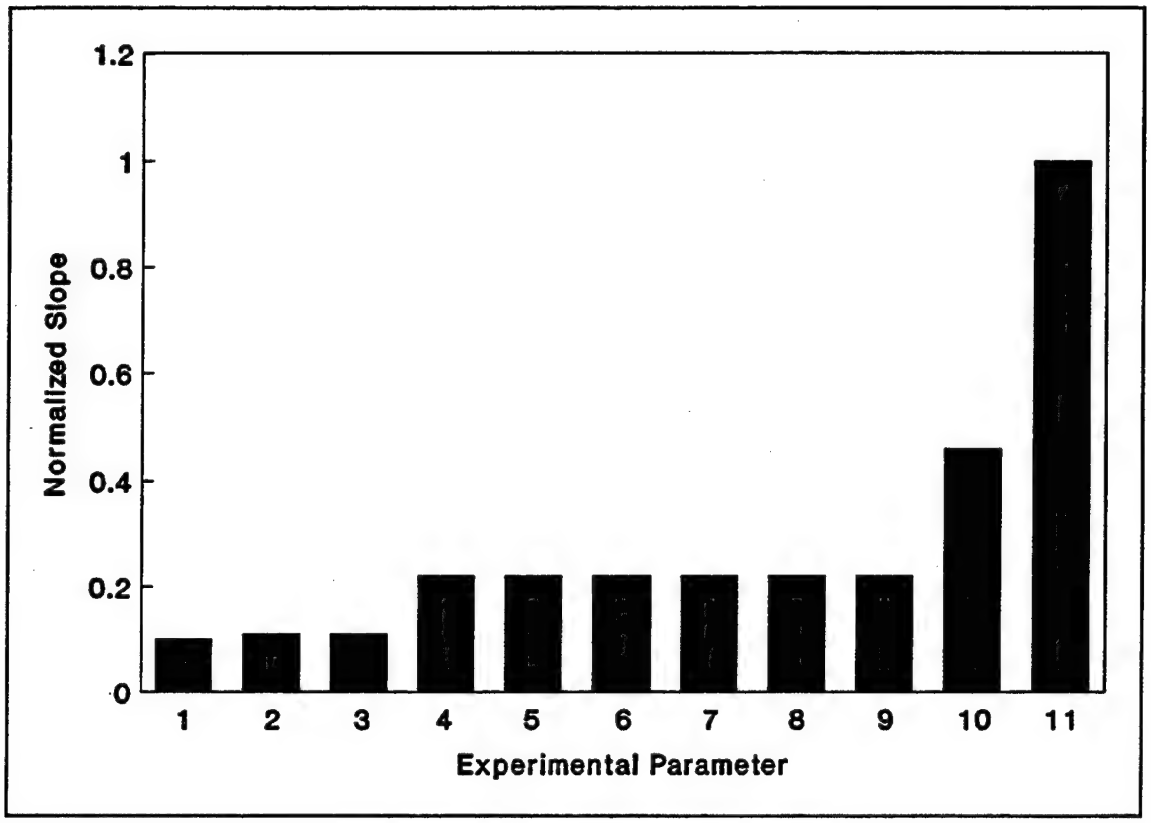

Fig. 2. Normalized average slopes of parameter sensitivity curves for $\langle \gamma \rangle$.

Parameters shown in Fig. 2:

1 -- Sample absorption
2 -- $I_{solution}$
3 -- I_{CS2}
4 -- $\chi^{(3)}_{CS2}$
5 -- Sample thickness
6 -- CS_2 thickness
7 -- Molecular weight
8 -- Sample mass
9 -- Sample volume
10-- n_{CS2}
11-- $n_{solution}$

RESULTS

A sampling of eight compounds evaluated for $\chi^{(3)}$ and $\langle\gamma\rangle$ reveals average $\chi^{(3)}$ and $\langle\gamma\rangle$ uncertainties of 8% and 9%, respectively, with values ranging from 6% to 10% for $\chi^{(3)}$ and 6% to 12% for $\langle\gamma\rangle$. In general, the lowest percent error is attributable to the highest voltage signal. Higher $\chi^{(3)}$ and $\langle\gamma\rangle$ values have higher associated phase-conjugate voltage readings and, therefore, lower percent uncertainties. For example, a material with a $\chi^{(3)}$ in the area of 10^{-9} will have a percent uncertainty of about 7% whereas a $\chi^{(3)}$ of 10^{-13} can have an uncertainty as high as 40%.

Table 4 shows the results obtained for zinc tetraphenyl tetrabenzporphyrin in tetrahydrafuran. It can be seen from these data that while the absolute uncertainty varies with concentration, the percent uncertainty remains relatively constant.

Table 4. Experimental results for zinc tetraphenyl tetrabenzporphyrin in tetrahydrafuran.

C (g/mL)	$\chi^{(3)}_{solution}$ ($\times10^{-13}$ esu)			$\chi^{(3)}_{solute}$ ($\times10^{-10}$ esu)			$\langle\gamma\rangle$ ($\times10^{-31}$ esu)		
0.00216	43.7	±1.78	(4%)	20.1	±0.82	(4%)	6.66	±0.38	(6%)
0.00076	14.5	±0.59	(4%)	18.8	±0.78	(4%)	6.26	±0.36	(6%)
0.00038	9.57	±0.39	(4%)	24.5	±1.04	(4%)	8.12	±0.48	(6%)
0.00019	6.34	±0.25	(4%)	32.1	±1.44	(4%)	10.6	±0.64	(6%)
0.00010	2.31	±0.09	(4%)	21.2	±1.14	(5%)	7.03	±0.48	(7%)
0	0.24	±0.01	(4%)	--		--	--		--

Figure 3 shows the curve fit data from Table 4 where $\chi^{(3)}_{solute}$ versus concentration is shown. The straight line is obtained by plotting Eq. 24 with $\chi^{(3)}_{solvent} = 2.4\times10^{-14}$ esu, $\chi^{(3)}_{solute} = 2.0\times10^{-9}$ esu, and the concentrations shown in Table 4. Specific values for $\chi^{(3)}_{solution}$ are compared in Table 5 to experimental values obtained from Table 4. Percent errors given in Table 5 are calculated with the assumption that the curve-fit values are the more correct. It is generally expected that experimental deviations from the curve-fit line will be within one or two standard deviations as given in Table 4, or at most about 10%. Absolute errors shown in Table 5, in two cases, are outside predicted uncertainty. It is currently believed that these relatively large percent errors are due to fluctuations in laser power; a variable which has not been considered in the uncertainty analysis. Variations, however, appear to be random and are expected to average out in the curve fitting process.

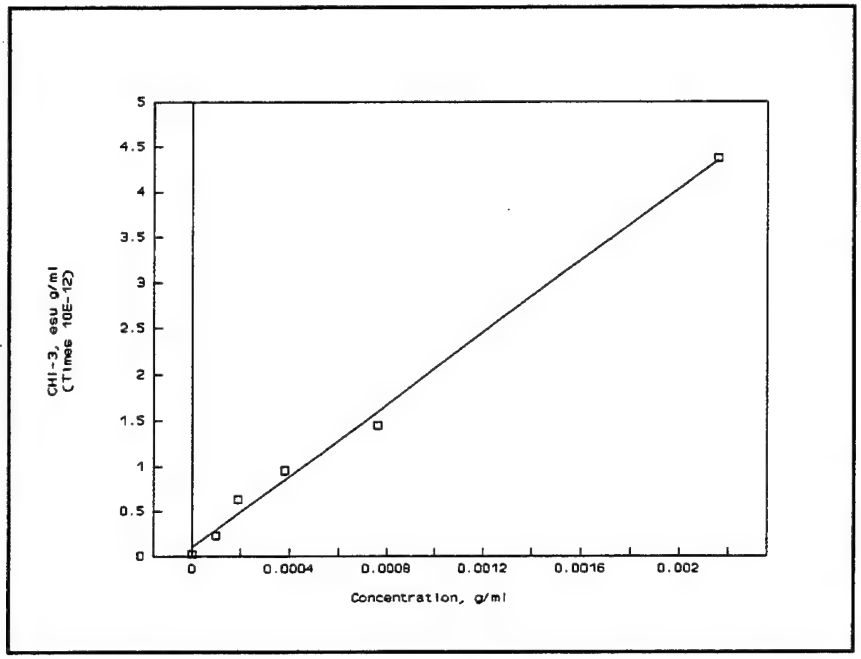

Fig. 3. Experimental data and curve-fit line versus concentration for zinc tetraphenyl tetrabenzporphyrin in tetrahydrafuran.

Table 5. Comparison of experimental and curve-fit data for zinc tetraphenyl tetrabenzporphyrin in tetrahydrafuran.

C (g/mL)	Experimental $\chi^{(3)}_{solution}$ ($\times 10^{-13}$ esu)	Curve-Fit $\chi^{(3)}_{solution}$ ($\times 10^{-13}$ esu)	Percent Error
0.00216	43.7	43	2%
0.00076	14.5	15	4%
0.00038	9.57	7.8	23%
0.00019	6.34	4.0	57%
0.00010	2.31	2.2	5%
0	0.24	0.24	0%

CONCLUSIONS AND RECOMMENDATIONS

Uncertainty expressions have been derived and used to evaluate a DFWM scheme used in the determination of third-order susceptibility and molecular second hyperpolarizability of nonlinear optical materials.

The results of a representative experimental run are presented showing that, for samples in solution, the greatest uncertainty is currently introduced by phase-conjugate voltage readings. As the strength of the phase-conjugate signal decreases, the overall experimental uncertainty increases. This relationship can occur as a result of a low laser output intensity or by the nonlinear material having a low phase-conjugate signal strength. Maximum experimental accuracy can be assured with proper laser maintenance and system alignment to optimize laser energy output and phase-conjugate signal strength.

Parameter sensitivity curves reveal that the indices of refraction of both the sample in solution and reference solution are the most critical parameters with respect to overall experimental uncertainty. Solution refractive indices are currently assumed equal to those of the solution solvent; the validity of this assumption should be verified in light of the results of this study.

Sensitivity plots contained in this report can be used as a general guide in estimating the impact of changes in tolerances of experimental variables. Accompanying software is now routinely used in DFWM experiments in determining $\chi^{(3)}$ and $\langle\gamma\rangle$ and their associated uncertainties.

Actual experimental deviations from a least-squares curve were shown to be within predicted uncertainties with the exception of some outliers attributable to variation in laser output power, which was not considered in the analysis.

Concerning the investigation of trends: results show that changes of ±10% percent or greater in $\chi^{(3)}$ and $\langle\gamma\rangle$ can be considered statistically significant. This confidence interval can be decreased by increasing the number of points (concentrations) used in the least-squares approximation.

The method of determining solution concentration outlined here has proven to be of acceptable accuracy (±1.6%) while also minimizing the production of hazardous waste and the time required to complete an experimental run.

It is believed that this study has given significant insight into the experimental uncertainties inherent to the DFWM technique when used in the evaluation of third-order susceptibility and molecular second hyperpolarizability of nonlinear optical materials.

REFERENCES

1. Rao, D.V.G.L.N., Aranda, F.J., Roach, J.F., Remy, D.E., *Appl. Phys. Lett.*, 1991, 58, 1241-1243.

APPENDICES

A. Derivation of Mass/Concentration Expression

B. Computer Program ERRCHI-3.BAS

C. Parameter Sensitivity Curves

APPENDIX A. Derivation of Mass/Concentration Expression

A technique has been developed to determine dilute solution concentrations from accurate weight measurements. The derivation is as follows:

An initial predetermined concentration C_i is prepared of weight m_i and density ρ. Some solution is removed for measurement and the sample is weighed again. This final weight is m_f. To determine the final volume V_f we can write:

$$V_f = \frac{m_f}{\rho}. \tag{A1}$$

The mass of the solute contained in V_f can be determined by the expression

$$m_{solute} = C_i V_f. \tag{A2}$$

Some solvent is added to dilute the solution for the next measurement. This new, added volume can be obtained by the expression

$$V_+ = \frac{m_n - m_f}{\rho}. \tag{A3}$$

The new concentration is

$$C_n = \frac{m_{solute}}{V_f + V_+}. \tag{A4}$$

Inserting Eqs. A1, A2 and A3 into Eq. A4, we obtain the expression

$$C_n = \frac{C_i \frac{m_f}{\rho}}{\frac{m_f}{\rho} + \frac{m_n - m_f}{\rho}}, \tag{A5}$$

which reduces to

$$C_n = C_i \frac{m_f}{m_n}. \tag{A5}$$

APPENDIX B. Program ERRCHI-3.BAS

```
10   REM  This program calculates CHI-3 and Gamma for samples in solution.
20   REM  It can be used in conjunction with Lotus spreadsheet CHI-3.WK1
30   REM  which uses a least-squares curve-fitting routine to determine
40   REM  solute CHI-3 values from solution CHI-3 values calculated
50   REM  with this program.   B. Kimball,  18 March 1994.
60
70   CLS
100  INPUT "I of solution (mv) = ", Isol
110  INPUT "I of CS2, (mv) = ", Ics
120  REM Ics = 50000
130  INPUT "Absorbance, = ", ab
140  INPUT "Concentration, (mg/ml) = ", con
143
144  REM              PARAMETERS FOR CHI-3 AND GAMMA EVALUATION

145  REM  Index of refraction of solution
147  ns = 1.44
150  REM  Path Length CS-2, (mm)
155  DCS = 2
160  REM  Path length solution, (mm)
162  DS = 2
165  REM  CHI-3 of Solvent, (esu)
167  Xsolv = 2.4E-14
168  REM  Uncertainty in Solvent CHI-3
170  WXsolv = 9.7E-16
172  REM  CHI-3 of CS-2
174  XCS = 6.8E-13
175  REM  Index of refraction of CS-2
180  ncs = 1.63
182  REM  Molecular weight of solute, g/mole
184  M = 678
186  REM  Avogadros number
188  A = 6.023E+23
190  REM  Mass of sample (mg)
195  mg = 3.8
200  REM  Volume of Solvent used in solution
205  ml = 5

210  REM                   PARAMETERS FOR CHI-3 UNCERTAINTY

220  PWXCS = 0
230  WXcs = XCS * PWXCS
240  PWIsol = .05
250  WIsol = Isol * PWIsol
260  PWIcs = .05
270  WIcs = Ics * PWIcs
280  PWns = .01
290  Wns = ns * PWns
300  PWncs = .001
310  Wncs = ncs * PWncs
320  PWDS = .001
330  WDS = DS * PWDS
340  PWDCS = .001
350  WDCS = DCS * PWDCS
360  PWab = .0008
370  Wab = ab * PWab
380  PWM = .001
390  WM = M * PWM
392  PWmg = .01
```

```
394  Wmg = mg * PWmg
396  PWml = .01
398  Wml = ml * PWml


400  REM              CALCULATE CHI-3 AND GAMMA

405  alpha = -LOG(10 ^ -ab)
410  P1 = Isol / Ics
420  P2 = ns / ncs
430  P3 = DCS / DS
440  P4 = (alpha / (1 - (EXP(-alpha)))) * EXP(alpha / 2)
450  Xsol = XCS * (P1 ^ .5) * (P2 ^ 2) * P3 * P4
460  Xsam = (Xsol - Xsolv) / (con / 1000)
470  L = (ns ^ 2 + 2) / 3
480  GAMMA = (Xsam * M) / (L ^ 4 * A)


490  REM            CALCULATE  Xsol UNCERTAINTY

495  REM   Sensitivity Expressions
500  SXcs = (P1 ^ .5) * (P2 ^ 2) * P3 * P4
510  SIsol = XCS * .5 * ((Isol ^ .5) ^ -1) * ((Ics ^ .5) ^ -1) *
      P2 ^ 2 * P3 * P4
520  SIcs = XCS * .5 * ((Isol ^ .5) / (Ics ^ 1.5)) * P2 ^ 2 * P3 * P4
530  Sns = XCS * (P1 ^ .5) * 2 * (ns / (ncs ^ 2)) * P3 * P4
540  Sncs = XCS * (P1 ^ .5) * ns ^ 2 * (2 / (ncs ^ 3)) * P3 * P4
550  SDCS = XCS * (P1 ^ .5) * (P2 ^ 2) * (1 / DS) * P4
560  SDS = XCS * (P1 ^ .5) * (P2 ^ 2) * (DCS / (DS ^ 2)) * P4
570  Sab = XCS * (P1 ^ .5) * P2 ^ 2 * P3 * ((1 - EXP(-alpha)) * ((alpha / 2) +
      EXP(alpha / 2)) - alpha * EXP(-alpha / 2)) / ((1 - EXP(-alpha)) ^ 2)

580  REM   Parameter Uncertainties
590  UXcs = SXcs * WXcs
600  UIsol = SIsol * WIsol
610  UIcs = SIcs * WIcs
620  Uns = Sns * Wns
630  Uncs = Sncs * Wncs
640  UDCS = SDCS * WDCS
650  UDS = SDS * WDS
660  Uab = Sab * Wab

670  REM Xsol Uncertainty
680  WXsol = (UXcs ^ 2 + UIsol ^ 2 + UIcs ^ 2 + Uns ^ 2 + Uncs ^ 2 +
      UDCS ^ 2 + UDS ^ 2 + Uab ^ 2) ^ .5


700  REM          CALCULATE con UNCERTAINTY

710  REM  Sensitivity Expressions
720  Smg = 1 / ml
730  Sml = mg / (ml ^ 2)

740  REM Parameter Uncertainties
750  Umg = Smg * Wmg
760  Uml = Sml * Wml

770  REM  con Uncertainty
780  Wcon = (Umg ^ 2 + Uml ^ 2) ^ .5
```

```
800  REM          CALCULATE Xsam UNCERTAINTIES

810  REM  Sensitivity Expressions
820  SXsol = 1000 / con
830  SXsolv = 1000 / con
840  Scon = 1000 * (Xsol - Xsolv) / (con ^ 2)

850  REM  Parameter Uncertainties
860  UXsol = SXsol * WXsol
870  UXsolv = SXsolv * WXsolv
880  Ucon = Scon * Wcon

890  REM  Xsam Uncertainty
900  WXsam = (UXsol ^ 2 + UXsolv ^ 2 + Ucon ^ 2) ^ .5


950  REM          CALCULATE L UNCERTAINTIES

960  REM  Sensitivity Expressions
970  SLn = 2 * ns / 3

980  REM  Parameter Uncertainties
990  ULn = SLn * Wns

1000 REM  L Uncertainty
1010 WL = ULn


1020 REM              CALCULATE GAMMA UNCERTAINTIES

1030 REM  Sensitivity Expressions
1040 SXsam = M / ((L ^ 4) * A)
1050 SM = Xsam / ((L ^ 4) * A)
1060 SL = 4 * Xsam * M / ((L ^ 5) * A)

1070 REM  Parameter Uncertainties
1080 UXsam = SXsam * WXsam
1090 UM = SM * WM
1100 UL = SL * WL

1110 REM  GAMMA Uncertainty
1120 WGAMMA = (UXsam ^ 2 + UM ^ 2 + UL ^ 2) ^ .5


1200 REM                    PRINT RESULTS

1204  PRINT "                      RESULTS"
1205  PRINT
1210  PRINT "CHI-3 of solution is"; Xsol
1220  PRINT "Uncertainty"; WXsol
1230  PRINT
1240  PRINT "CHI-3 of sample is"; Xsam
1250  PRINT "Uncertainty"; WXsam
1260  PRINT
1270  PRINT "Gamma of the solute is"; GAMMA
1280  PRINT "Uncertainty"; WGAMMA
```

```
1310  PRINT "              PARAMETER UNCERTAINTIES"
1320  PRINT
1330  PRINT "                        Xsol"
1340  PRINT "CHI-3 of CS2 "; UXcs
1350  PRINT "Voltage reading for solution"; UIsol
1360  PRINT "Voltage reading for CS2"; UIcs
1370  PRINT "Solution refractive index"; Uns
1380  PRINT "CS2 refractive index"; Uncs
1390  PRINT "Solution thickness"; UDS
1400  PRINT "CS2 thickness"; UDCS
1410  PRINT "Absorption"; Uab
1415  INPUT ; "Hit Return", me
1416  CLS
1420  PRINT
1430  PRINT "                   Concentration"
1440  PRINT "Weight"; Umg
1450  PRINT "Volume"; Uml
1470  PRINT
1480  PRINT "                         Xsam"
1490  PRINT "Solution CHI-3"; UXsol
1500  PRINT "Solvent CHI-3"; UXsolv
1510  PRINT "Concentration"; Ucon
1520  PRINT
1530  PRINT "                   Field Factor L"
1540  PRINT "Solution refractive index"; ULn
1550  PRINT
1560  PRINT "                        GAMMA"
1570  PRINT "Sample CHI-3"; UXsam
1580  PRINT "Molecular weight"; UM
1590  PRINT "Field Factor L"; UL
1700  END
```

APPENDIX C. Parameter Sensitivity Curves.

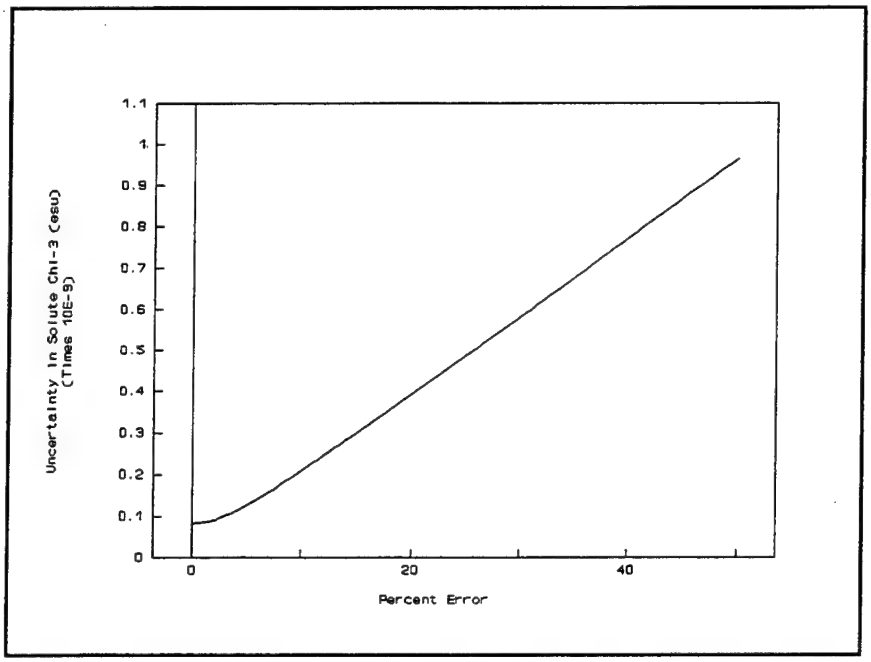

Fig. C1. Uncertainty in $\chi^{(3)}$ resulting from percent error in the assumed value for the $\chi^{(3)}$ of CS_2.

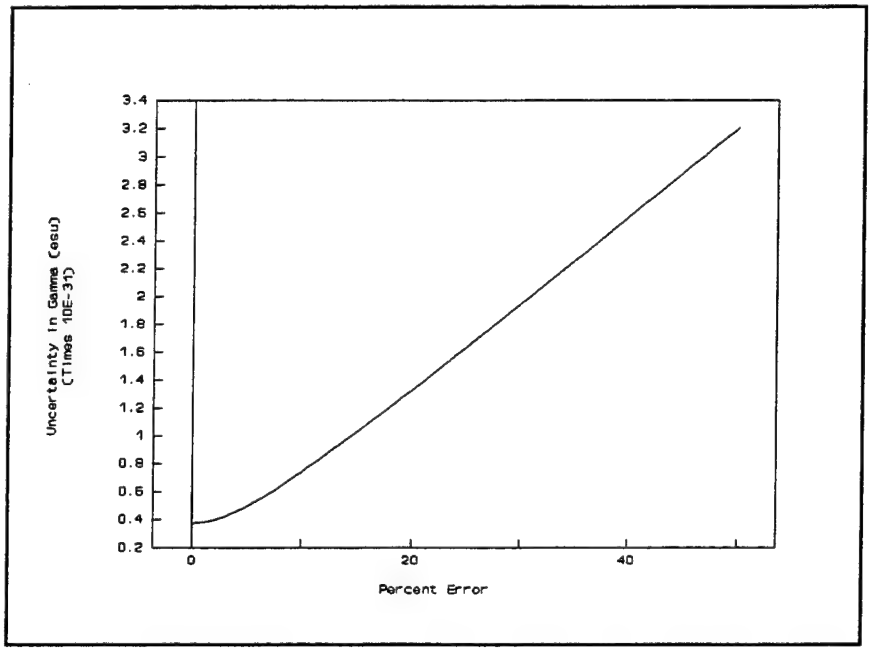

Fig. C2. Uncertainty in $\langle\gamma\rangle$ resulting from percent error in the assumed value for the $\chi^{(3)}$ of CS_2.

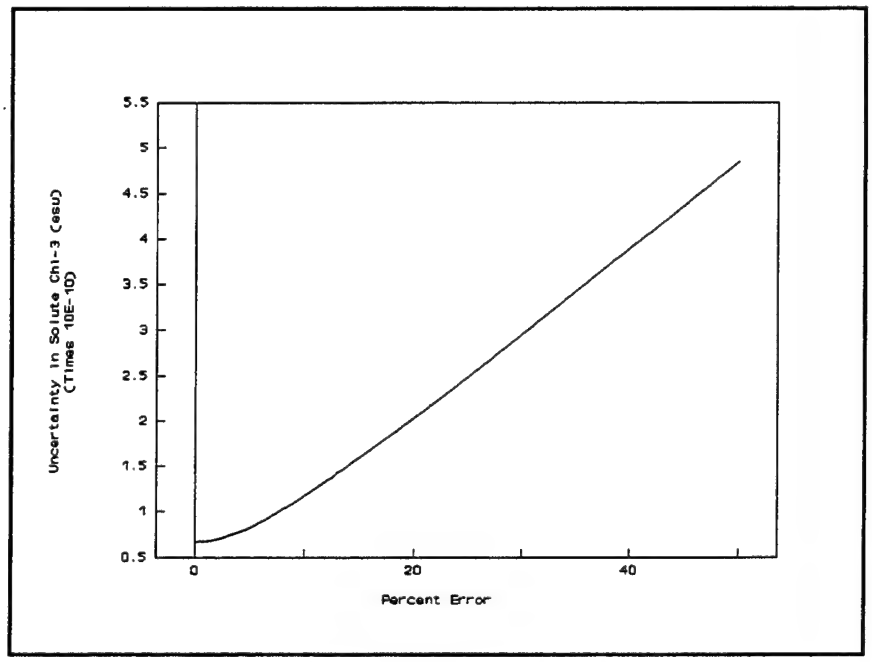

Fig. C3. Uncertainty in $\chi^{(3)}_{solute}$ resulting from percent error in the DFWM phase-conjugate signal of the solution.

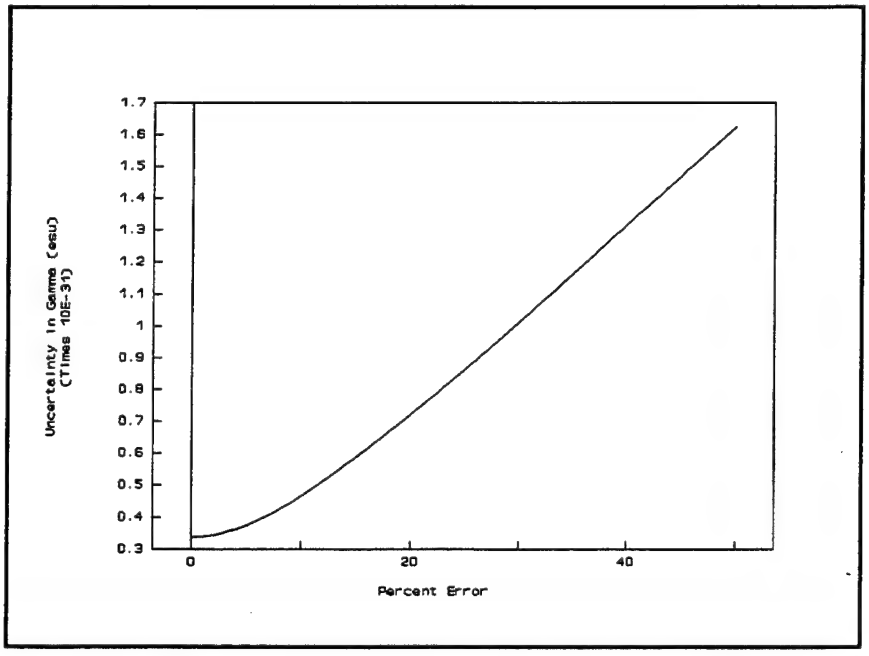

Fig. C4. Uncertainty in $\langle\gamma\rangle$ resulting from percent error in the DFWM phase-conjugate signal of the solution.

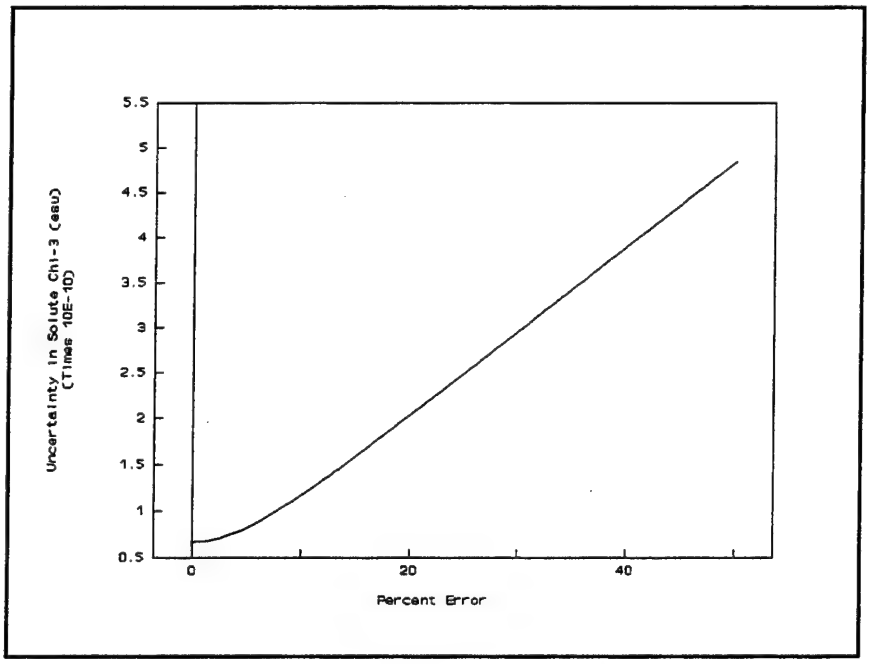

Fig. C5. Uncertainty in $\chi^{(3)}_{solute}$ resulting from percent error in the DFWM phase-conjugate signal of CS_2.

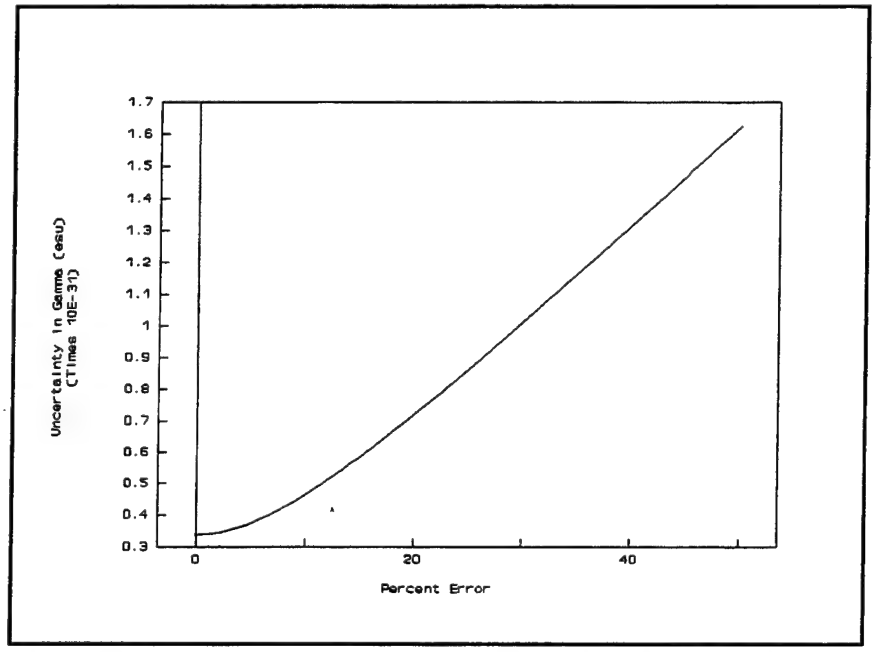

Fig. C6. Uncertainty in $\langle\gamma\rangle$ resulting from percent error in the DFWM phase-conjugate signal of CS_2.

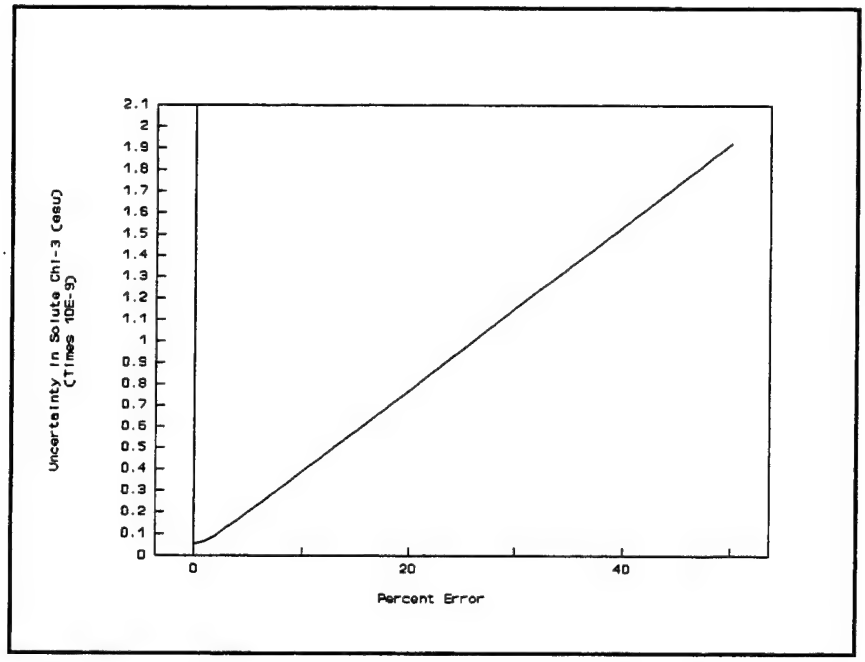

Fig. C7. Uncertainty in $\chi^{(3)}_{solute}$ resulting from percent error in the index of refraction of the solution.

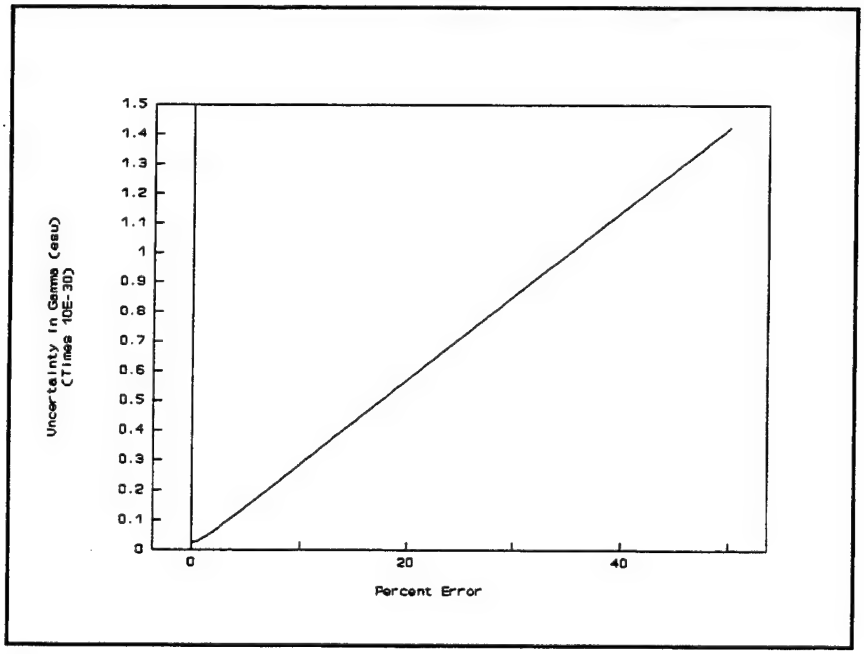

Fig. C8. Uncertainty in $\langle\gamma\rangle$ resulting from percent error in the index of refraction of the solution.

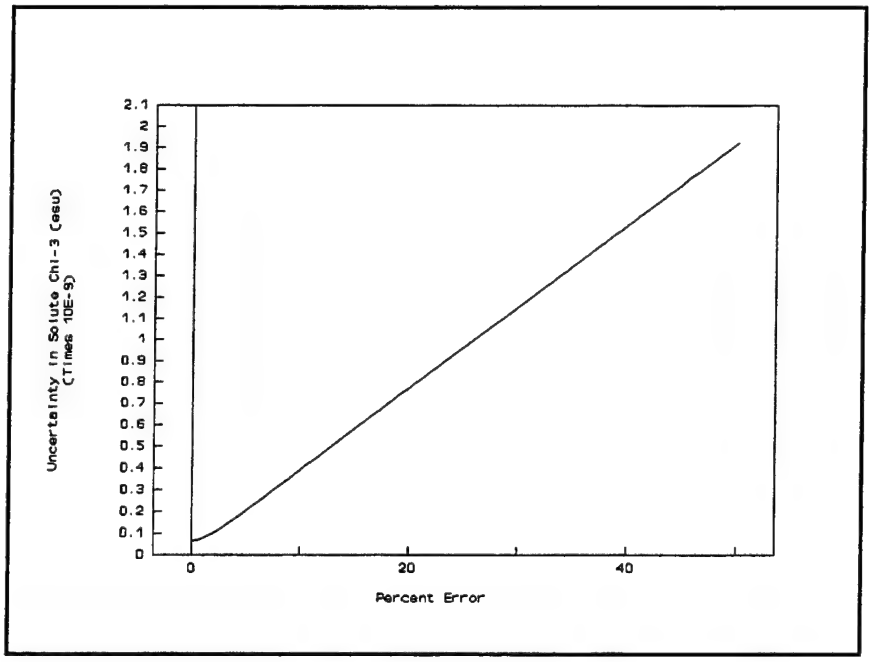

Fig. C9. Uncertainty in $\chi^{(3)}_{solute}$ resulting from percent error in the index of refraction of CS_2.

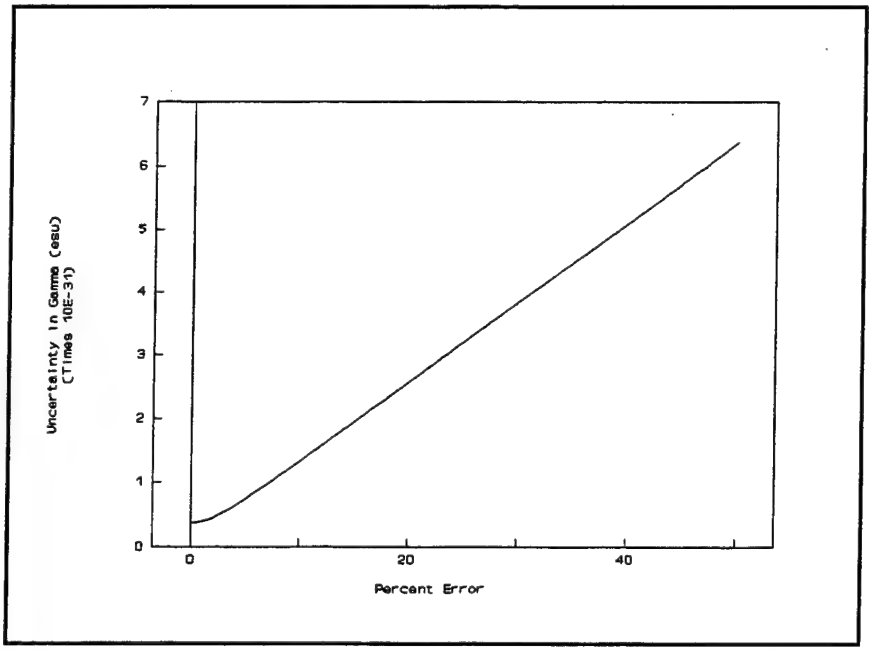

Fig. C10. Uncertainty in $\langle\gamma\rangle$ resulting from percent error in the index of refraction of CS_2.

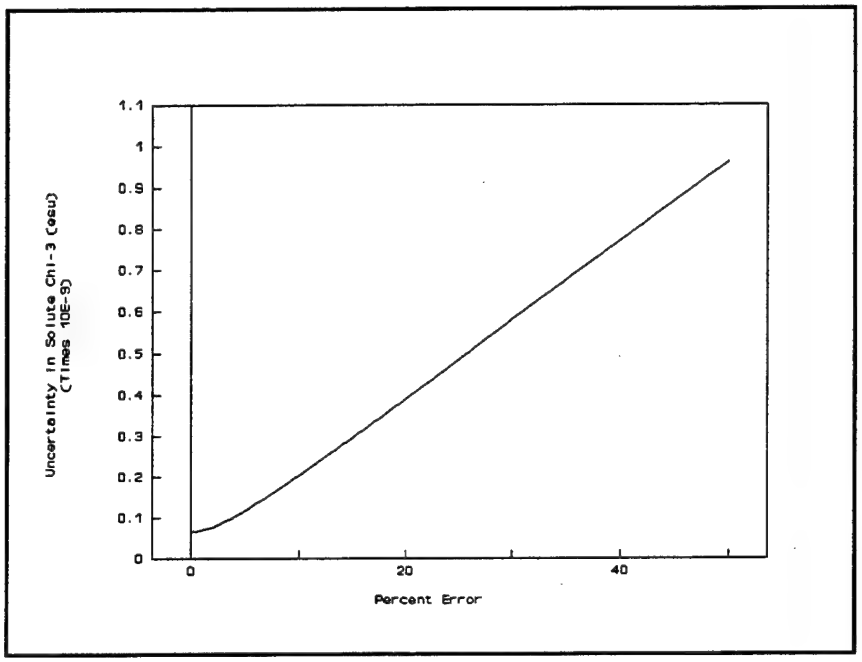

Fig. C11. Uncertainty in $\chi^{(3)}_{solute}$ resulting from percent error in sample thickness.

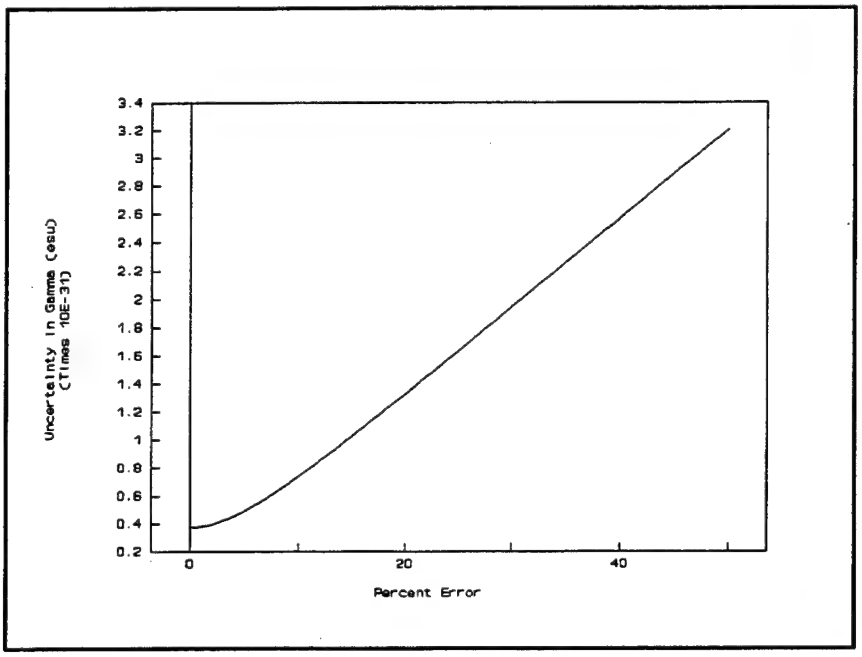

Fig. C12. Uncertainty in $\langle\gamma\rangle$ resulting from percent error in sample thickness.

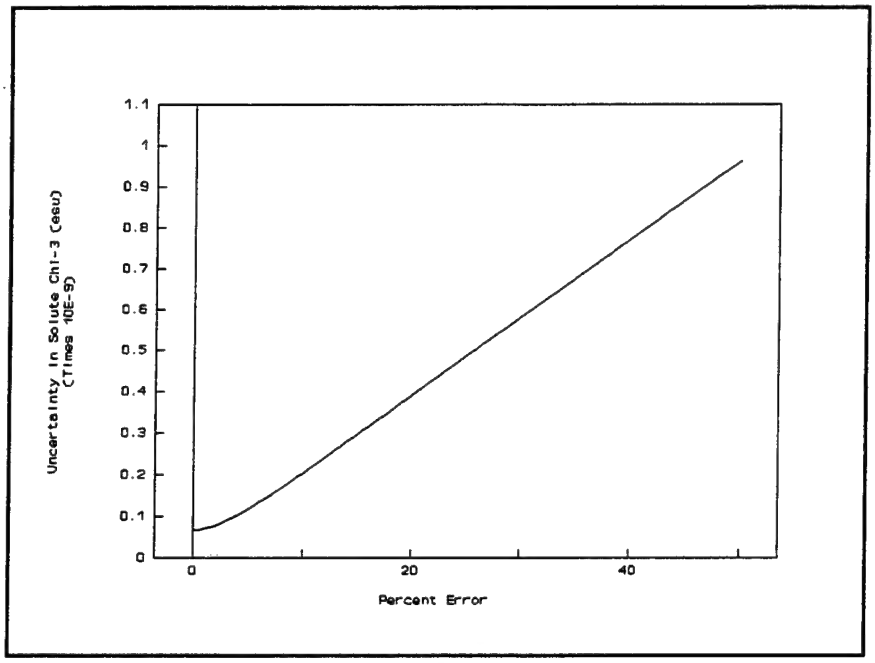

Fig. C13. Uncertainty in $\chi^{(3)}_{solute}$ resulting from percent error in CS_2 thickness.

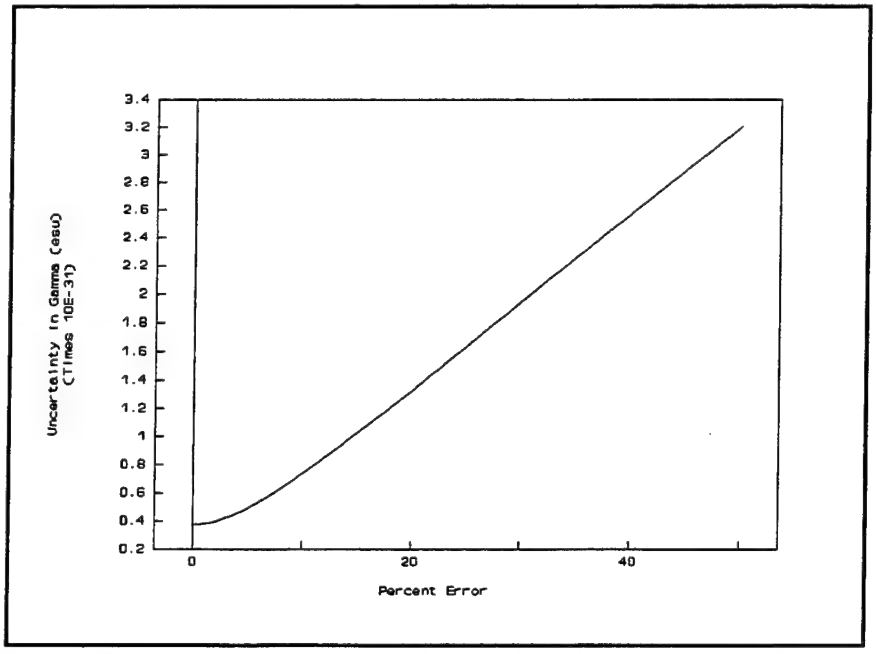

Fig. C14. Uncertainty in $\langle\gamma\rangle$ resulting from percent error in CS_2 thickness.

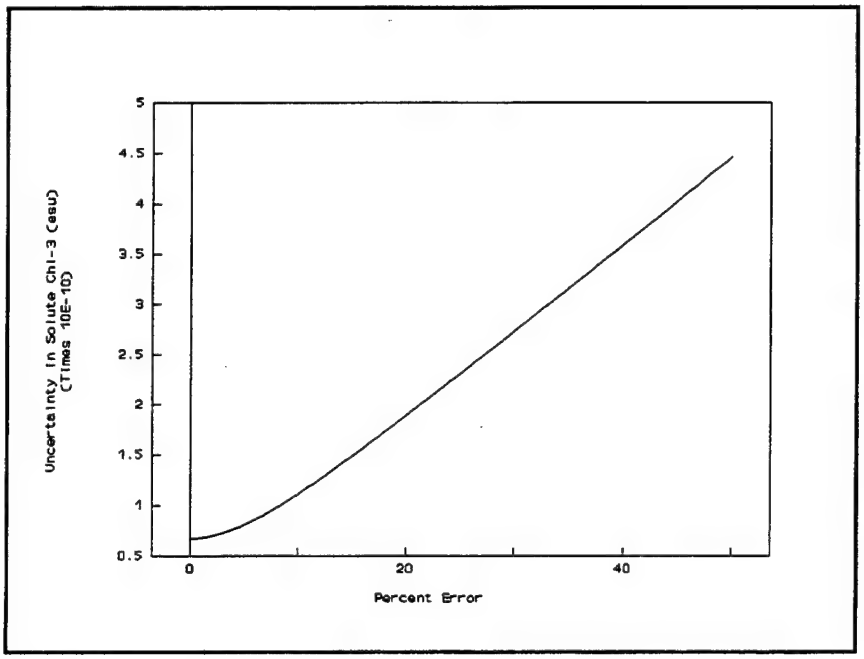

Fig. C15. Uncertainty in $\chi^{(3)}_{solute}$ resulting from percent error in sample absorption.

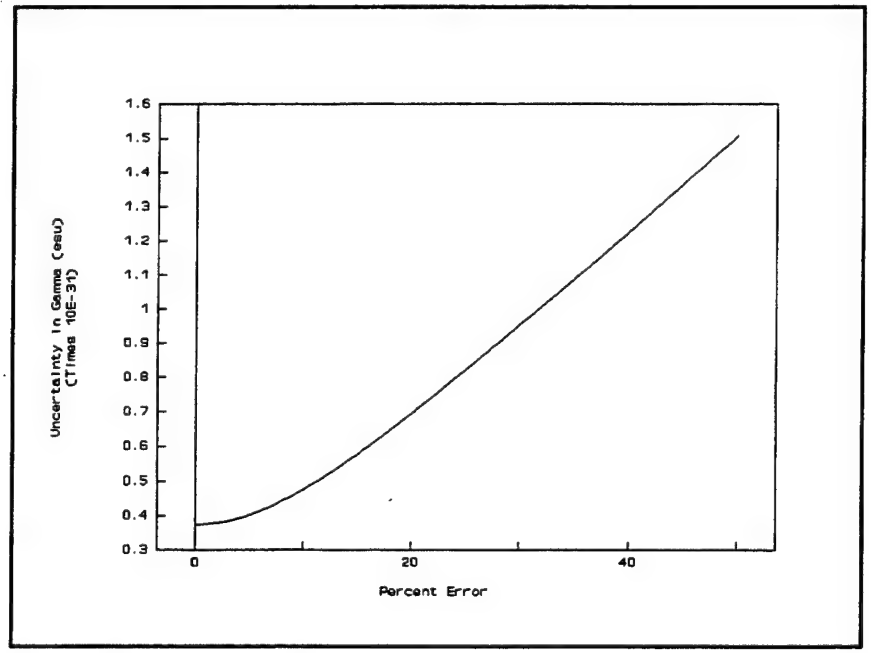

Fig. C16. Uncertainty in $\langle\gamma\rangle$ resulting from percent error in sample absorption.

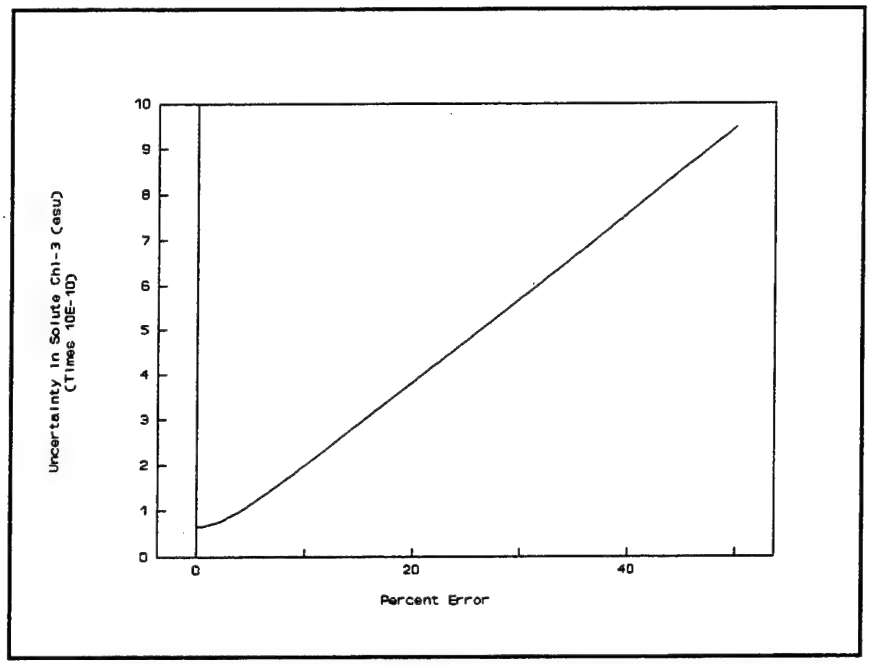

Fig. C17. Uncertainty in $\chi^{(3)}_{solute}$ resulting from percent error in measurement of solution weight.

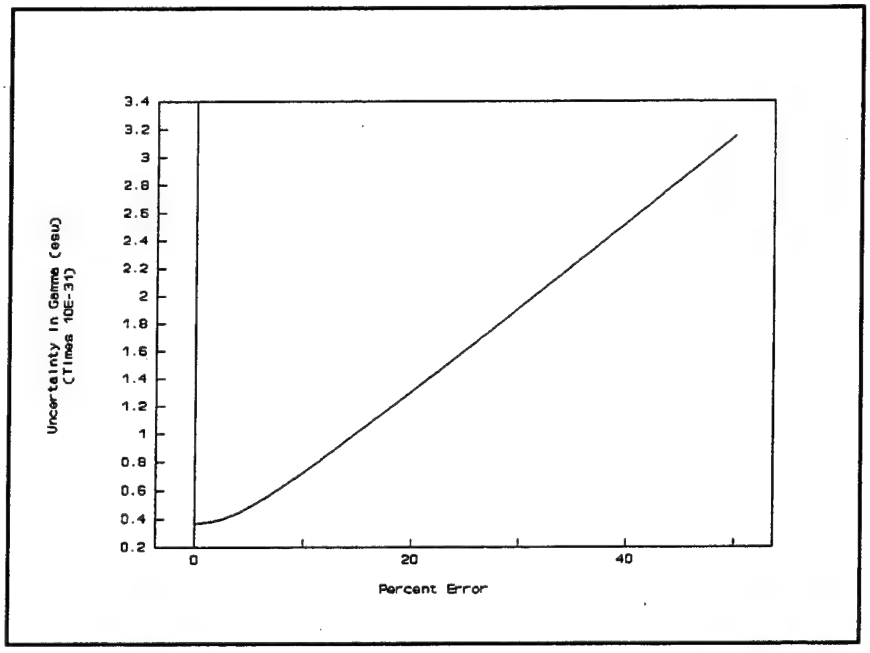

Fig. C18. Uncertainty in $\langle\gamma\rangle$ resulting from percent error in measurement of solution weight.

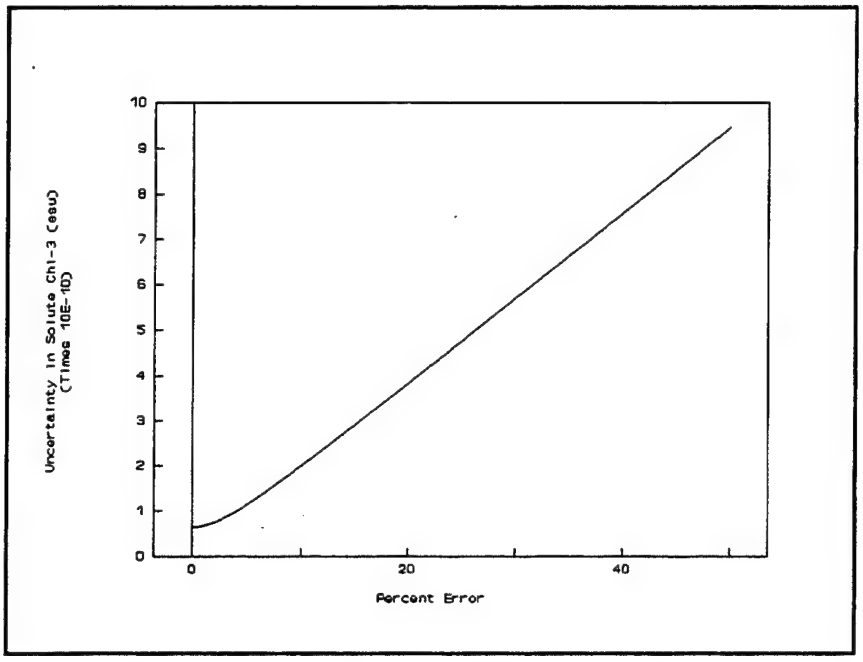

Fig. C19. Uncertainty in $\chi^{(3)}_{solute}$ resulting from percent error in measurement of solution volume.

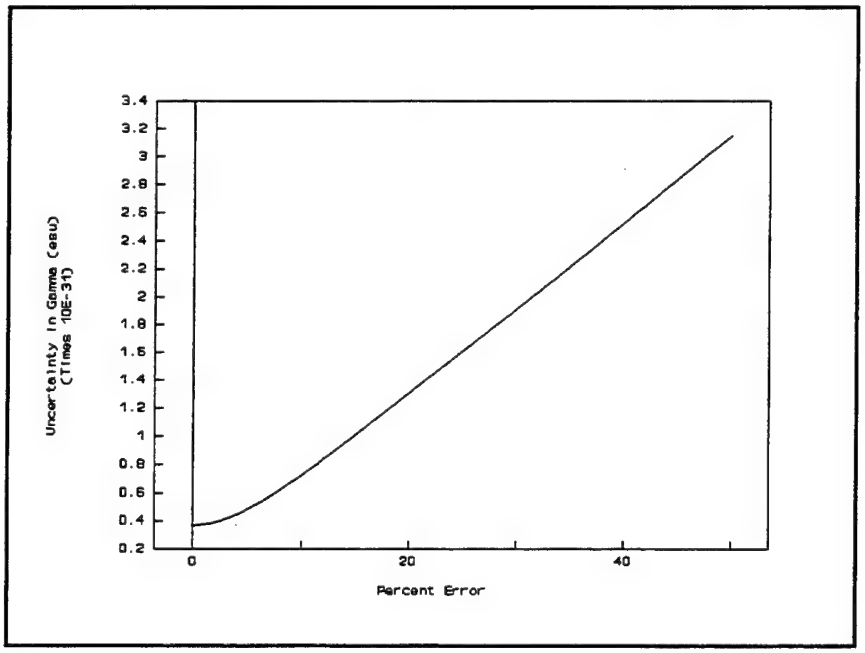

Fig. C20. Uncertainty in $\langle\gamma\rangle$ resulting from percent error in measurement of solution volume.

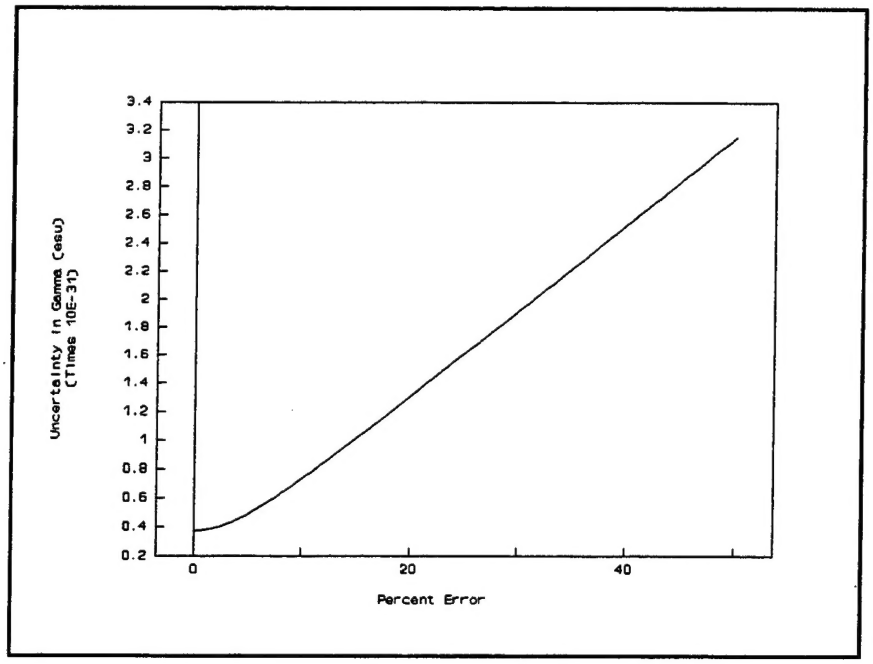

Fig. C21. Uncertainty in $\langle \gamma \rangle$ resulting from percent error in molecular weight of solute.

DISTRIBUTION LIST

1 copy to:

COMMANDER
U.S. ARMY TRAINING AND DOCTRINE
COMMAND
ATTN: ATCD-SE
FT. MONROE, VA 23651

1 copy to:

PROGRAM MANAGER - CLOTHING AND
INDIVIDUAL EQUIPMENT
ATTN: AMCPM-CIE
WOODBRIDGE, VA 22194-4206

1 copy to:

COMMANDANT
U.S. ARMY INFANTRY SCHOOL
ATTN: ATSH-CD-MLS-C
FT. BENNING, GA 31905

1 copy to:

COMMANDANT
U.S. ARMY ARMOR SCHOOL
ATTN: ATSB-CD-ML
FT. KNOX, KY 40121-5215

1 copy to:

COMMANDANT
U.S. ARMY CHEMICAL SCHOOL
ATTN: ATZN-CM-CS
FT. McCLELLAN, AL 36205-5000

1 copy to:

COMMANDANT
U.S. ARMY AVIATION SCHOOL
ATTN: ATZQ-CDM-C
FT. RUCKER, AL 36362

1 copy to:

COMMANDER
U.S. ARMY NUCLEAR AND
CHEMICAL AGENCY
ATTN: MONA-NU BLDG. 2073
7500 BACKLICK ROAD
SPRINGFIELD, VA 22150-3198

1 copy to:

COMMANDER
U.S. ARMY NUCLEAR AND
CHEMICAL AGENCY
ATTN: MONA-ZB BLDG.2073
7500 BACKLICK ROAD
SPRINGFIELD, VA 22150-3198

1 copy to:

DIRECTOR
DEFENSE NUCLEAR AGENCY
ATTN: TDTR
6801 TELEGRAPH ROAD
ALEXANDRIA, VA 23310-3398

1 copy to:

DIRECTOR
DEFENSE NUCLEAR AGENCY
ATTN: HRP
6801 TELEGRAPH ROAD
ALEXANDRIA, VA 23310-3398

1 copy to:

HQDA
OFFICE OF THE SURGEON GENERAL
ATTN: DASG-HCG
5109 LEESBURG PIKE
FALLS CHURCH, VA 22041-3258

1 copy to:

COMMANDER
U. S. ARMY COMBINED ARMS DEFENDE CENTER
ATTN: ATZL-CAD-N
FT. LEAVENWORTH,KS 66027-5300

1 copy to:

U.S. ARMY AVIATION MEDICAL RESEARCH
LABORATORY
ATTN: SGRD-VAB-CB
FT. RUCKER, AL 36352-5000

1 copy to:

COMMANDER
WALTER REED INSTITUTE OF RESEARCH
ATTN: SGRD-UWZ
WASHINGTON, DC 20307-5100

1 copy to:

U.S. ARMY RESEARCH LABORATORY
ATTN: SLCHD-NW-TN
2800 POWDER MILL ROAD
ADELPHI, MD 20783

1 copy to:

U.S. NAVY CLOTHING AND TEXTILE
RESEARCH FACILITY
ATTN: CODE 40.1
21 STRATHMORE ROAD
NATICK, MA 01760-2490

2 copies to:

DEFENSE TECHNICAL INFORMATION CENTER
CAMERON STATION
ALEXANDRIA, VA 22314

7 copies to:

COMMANDER
U.S. ARMY NATICK RD & E CENTER
TECHNICAL LIBRARY
ATTN: STRNC-MIL
NATICK, MA 01760

1 copy to:

COMMANDER
U.S. ARMY NATICK RD & E CENTER
ATTN: STRNC-MSR
NATICK, MA 01760-5020

50 copies to:

COMMANDER
U.S. ARMY NATICK RD & E CENTER
ATTN: STRNC-YSD (Mr. Kimball)
NATICK, MA 01760-5020